J|A|C|S ARTICLES

Published on Web 02/23/2010

Cooperative Effects in Ternary Cu−Ni−Fe Catalysts Lead to Enhanced Alkene Selectivity in Alkyne Hydrogenation

Blaise Bridier[†] and Javier Pérez-Ramírez*[,†,‡,§]

Institute of Chemical Research of Catalonia (ICIQ), Avinguda dels Països Catalans 16, 43007 Tarragona, Spain, and Catalan Institution for Research and Advanced Studies (ICREA), Passeig de Lluís Companys 23, 08010 Barcelona, Spain

Received December 3, 2009; E-mail: jpr@chem.ethz.ch

Abstract: A new generation of heterogeneous Cu−Ni−Fe catalysts with appropriate metal ratios displayed outstanding alkene selectivity in the gas-phase hydrogenation of propyne ($S(C_3H_6)$ up to 100%) and ethyne ($S(C_2H_4)$ up to 80%). The design was accomplished by orchestrating key functions in the catalyst: copper is the base hydrogenation metal, nickel increases the hydrogen coverage to minimize oligomerization, and iron acts as structural promoter. In addition to the largely improved alkene selectivity compared to that of the commonly applied Pd catalysts, the ternary Cu−Ni−Fe catalysts promise substantial process advantages, since they do not require CO feeding as selectivity enhancer and they yield high alkene selectivity in a broad window of H_2/alkyne ratios. The ternary system requires higher operating temperatures compared to those for palladium.

Introduction

The production of light olefins (ethylene and propylene), namely by steam cracking, generates impurities of acetylenics and diolefins as byproducts. For example, the C2 cut typically contains 0.5−3% of ethyne and the C3 cut contains 2−8% of propyne and propadiene.[1] Reducing the level of these highly unsaturated compounds to <5 ppm is required to fulfill the stringent specifications for both chemical- and polymer-grade olefins. The partial hydrogenation of alkynes and alkadienes over promoted Pd/Al_2O_3 or Pd/SiO_2 catalysts with a low palladium loading (<0.05 wt %) is widely used for upgrading olefin streams.[2] The reaction is carried out in the gas phase for C2 and C3 cuts and in the liquid phase for C3, C4, and heavier cuts.[1] The alkene selectivity in gas-phase alkyne hydrogenation over pure palladium in supported or unsupported forms is generally too low[3] to justify its implementation in industry. Therefore, modification of the Pd catalyst by a second metal such as Ag or Au and/or by continuous CO feeding comprise imperative actions to increase the alkene selectivity.[2] Despite these modifications, overhydrogenation to the alkane and especially oligomerization to higher hydrocarbons (called green oil) remain the major drawbacks of industrial palladium catalysts. In particular, green oil causes operating problems such as shorter cycles due to catalyst fouling, the need for regeneration, and plugging of piping.[1] In addition, intensive separation processes of the green oil and the alkane from the alkene are required downstream of the hydrogenation reactors. For example, a state-of-the-art Pd−Ag catalyst in ethyne hydrogenation under simulated tail-end conditions led to 45% ethene selectivity, 28.8% ethane selectivity, and 26.2% green oil selectivity at nearly complete ethyne and hydrogen conversion.[4] In another publication, average ethylene selectivity of 40% was reported in commercial plants over promoted Pd/SiO_2.[5] The statement by Somorjai[6] that "the focus of catalysis research in the 21st century should be on achieving 100% selectivity for the desired product" is clearly applicable to industrial alkyne hydrogenation.

Recent work on alkyne hydrogenation related to olefin purification has chiefly covered different aspects of Pd-based catalysts,[3c,7] including particle size and support effects, the influence of modifiers, and the interplay of hydride and carbide phases on the alkene vs alkane selectivity. Fewer efforts have

[†] ICIQ.
[‡] ICREA.
[§] Current address: Institute for Chemical and Bioengineering, Department of Chemistry and Applied Biosciences, ETH Zurich, CH-8093 Zurich, Switzerland.

(1) (a) Derrien, M. L. In *Catalytic Hydrogenation*; Červený, L., Ed.; Studies in Surface Science and Catalysis; Elsevier: Amsterdam, 1986; Vol. 27, p 613.
(2) (a) Rase, H. F. *Handbook of Commercial Catalysts*; CRC Press: Boca Raton, FL, 2000; p 137. (b) Bond, G. C. *Metal-Catalysed Reactions of Hydrocarbons*; Springer: New York, 2005; p 395. (c) Borodziński, A.; Bond, G. C. *Catal. Rev.-Sci. Eng.* **2006**, *48*, 91–144.
(3) (a) Molero, H.; Bartlett, B. F.; Tysoe, W. T. *J. Catal.* **1999**, *181*, 49–56. (b) Molnár, Á.; Sárkány, A.; Varga, M. *J. Mol. Catal. A: Chem.* **2001**, *173*, 185–221. (c) Kovnir, K.; Osswald, J.; Armbrüster, M.; Teschner, D.; Weinberg, G.; Wild, U.; Knop-Gericke, A.; Ressler, T.; Grin, Y.; Schlögl, R. *J. Catal.* **2009**, *264*, 93–103.
(4) Molinier, M.; Ou, J. D.-Y.; Risch, M. A. U.S. Patent 2004176651, 2004. The commercial supported Pd−Ag catalyst (G-58C from Süd Chemie) was tested at $T = 373$ K, $P = 2068$ kPa, GHSV = 4500 h^{-1}, and $H_2/C_2H_2 = 1.3$. The hydrocarbon feed contained 1.65 mol % ethyne, 70 mol % ethene, and the balance nitrogen.
(5) Büchele, W.; Roos, H.; Wanjek, H.; Müller, H. J. *Catal. Today* **1996**, *30*, 33–39.
(6) Somorjai, G. A.; Borodko, Y. G. *Catal. Lett.* **2001**, *76*, 1–5.
(7) (a) López, N.; Bridier, B.; Pérez-Ramírez, J. *J. Phys. Chem. C* **2008**, *112*, 9346–9350. (b) Ruta, M.; Semagina, N.; Kiwi-Minsker, L. *J. Phys. Chem. C* **2008**, *112*, 13635–13641. (c) Studt, F.; Abild-Pedersen, F.; Bligaard, T.; Sørensen, R. Z.; Christensen, C. H.; Nørskov, J. K. *Angew. Chem., Int. Ed.* **2008**, *47*, 9299–9302. (d) Teschner, D.; Borsodi, J.; Wootsch, A.; Révay, Z.; Hävecker, M.; Knop-Gericke, A.; Jackson, D. S.; Schlögl, R. *Science* **2008**, *320*, 86–89. (e) Teschner, D.; Révay, Z.; Borsodi, J.; Hävecker, M.; Knop-Gericke, A.; Schlögl, R.; Milroy, D.; Jackson, D. S.; Torres, D.; Sautet, P. *Angew. Chem., Int. Ed.* **2008**, *47*, 9274–9278. (f) Mei, D.; Neurock, M.; Smith, C. M. *J. Catal.* **2009**, *268*, 181–195.

been paid to develop alternative systems that exceed the selectivity of commercial palladium catalysts under realistic process conditions. It is known that supported gold nanoparticles display alkene selectivity >80% in the gas-phase hydrogenation of ethyne and propyne,[8] although a catalyst deprived of expensive noble metals is highly preferred from a cost standpoint. Studt et al.[9] identified that, in contrast to pure Ni, Ni−Zn alloys supported on $MgAl_2O_4$ did not produce ethane during ethyne hydrogenation, implying its highly selective character. However, nothing was mentioned about the oligomeric byproduct and no absolute value of ethene selectivity was stated. In previous results over related Ni−Al and Ni−Zn−Al catalysts,[10] extensive green oil production was observed. Activated Cu−Al hydrotalcites and Cu/SiO_2 exhibited up to 80% propene selectivity and no propane formation in propyne hydrogenation.[11] However, the selectivity to oligomers amounted to ≥20%, particularly below 450 K, and the catalysts deactivate quickly due to extensive coking.[10a,11] Therefore, existing copper catalysts are not attractive for implementation either. The combination of nickel and copper in a quaternary $Ni_{0.5}Cu_{0.5}Zn_1Al_2$ catalyst was evaluated by Rodríguez et al.[10a] without much success; ethene selectivity of 40% was maximally achieved at a low degree of ethyne conversion (14%).

The above analysis stresses that the challenge to identify a competitive catalyst for partial alkyne hydrogenation in general and for the purification of olefin streams in particular requires suppressing *both* overhydrogenation and oligomerization channels. Herein we report a novel family of ternary Cu−Ni−Fe catalysts with outstanding alkene selectivity in the gas-phase hydrogenation of propyne and ethyne with or without excess alkene in the feed. The design comprised the incorporation of components with complementary functions in the heterogeneous catalyst: copper as the base hydrogenation metal, optimized amounts of nickel to increase the hydrogen coverage and to minimize the characteristic oligomerization of pure copper, and iron as an enhancer of the fraction of exposed copper and nickel sites. The crucial role of iron was assessed by direct comparison of Cu−Ni−Fe catalysts with Cu−Ni−Al analogues. To our knowledge, the combination of these three metals and the resulting selectivity to the double bond find no precedence in the existing literature. In addition to the superior selectivity, the Cu−Ni−Fe catalysts bring attractive process advantages with respect to palladium catalysts, as the former require no CO feeding and operate selectively in a wide range of H_2/alkyne ratios.

Experimental Section

The catalyst precursors $Cu_{3-x}Ni_xFe$ and $Cu_{3-x}Ni_xAl$ ($x = 0-3$) were synthesized by continuous coprecipitation using the in-line deposition precipitation (ILDP) method.[12] Aqueous solutions of the corresponding metal nitrates in the desired ratios and the precipitating agent ($NaOH + Na_2CO_3$, 1 M of each) were pumped into a 6 cm^3 reactor attached to a high-shear homogenizer rotating at 13 500 rpm. The pH of the slurry was measured and controlled by an in-line probe directly at the outlet of the precipitation chamber. The coprecipitation was carried out at pH 9 with an average residence time of 18 s. The precipitate slurry was aged at 313 K for 12 h, filtered, washed with deionized water, and dried at 353 K for 12 h. The solid was calcined in static air at 873 K for 15 h using a heating rate of 5 K min^{-1}.

The chemical composition of the solids was determined by X-ray fluorescence in a Philips PW 2400 spectrometer. Powder X-ray diffraction was studied in a Bruker AXS D8 Advance diffractometer equipped with a Cu tube, a Ge(111) incident beam monochromator ($\lambda = 0.1541$ nm), and a Vantec-1 PSD. Data were recorded in the range of 5−70° 2θ with a step size of 0.02° and a counting time of 4 s per step. N_2 isotherms at 77 K were measured in a Quantachrome Autosorb-1-MP analyzer. Prior to analysis, the samples were degassed under vacuum at 573 K for 12 h. Temperature-programmed reduction with hydrogen (H_2-TPR) was measured in a Thermo Scientific TPDRO 1100 setup equipped with a thermal conductivity detector. The sample (ca. 10 mg) was loaded in the quartz microreactor (11 mm i.d.), pretreated in N_2 (20 cm^3 min^{-1}) at 573 K for 30 min, and cooled to 323 K under the same atmosphere. The analysis was carried out in a mixture of 5 vol % H_2/N_2 (20 cm^3 min^{-1}), ramping the temperature from 323 to 1173 at 10 K min^{-1}. X-ray photoelectron spectroscopy (XPS) measurements were obtained using a VG-Microtech Multilab 3000 spectrometer equipped with Mg Kα ($h\nu = 1253.6$ eV) and Al Kα ($h\nu = 1486.6$ eV) excitation sources, a nine-channeltron detection system, and a hemispheric electron analyzer. The sample was outgassed overnight at room temperature in a UHV chamber (<5 × 10^{-8} Torr). All binding energies were referenced to the C 1s line at 284.6 eV, and the integrated intensities were corrected by atomic sensitivity factors.

The gas-phase hydrogenation of alkynes was studied at ambient pressure in a quartz fixed-bed microreactor (12 mm i.d.) using a catalyst mass of 0.15 g (sieve fraction 200−400 μm) and a total gas flow of 42 cm^3 min^{-1} (space velocity (*SV*) 16 800 cm^3 g^{-1} h^{-1}). The samples were pretreated in He at 573 K and reduced in 5 vol % H_2/He at 773 K for 30 min. Isothermal tests were carried out at 423−523 K using the following feed mixtures: 2.5/7.5/90 $C_3H_4(C_2H_2)$/H_2/He and 1.5/8.1/4.5/85.9 $C_3H_4(C_2H_2)/C_3H_6(C_2H_4)/H_2$/He. Each temperature was typically held for a period of 5 h. Heating and cooling ramps of 5 K min^{-1} were used in all the steps. The stability of the optimal catalyst was evaluated in the above alkyne + alkene mixtures at 523 K during 30 h. The influence of the hydrogen-to-alkyne ratio (H_2/alkyne = 1−12) was studied at 523 K. In these tests, the inlet alkyne concentration was kept at 2.5 vol % and the H_2 concentration was progressively decreased from 30 to 2.5 vol % by balancing the mixture with He in order to keep the total flow constant. Propyne, ethyne, propene, ethene, propane, and ethane were analyzed online using an Agilent GC6890N gas chromatograph equipped with a GS-GasPro column and a thermal conductivity detector. The selectivity to the alkene (alkane) was determined as the amount of alkene (alkane) formed divided by the amount of reacted alkyne. The selectivity to oligomers was obtained as: $S(\text{oligomers}) = 1 - S(\text{alkene}) - S(\text{alkane})$.

Results and Discussion

The $Cu_{3-x}Ni_xFe$ and $Cu_{3-x}Ni_xAl$ precursors with $x = 0-3$ were synthesized by continuous coprecipitation at pH 9. The molar Cu/Ni/Fe and Cu/Ni/Al ratios in the samples determined by X-ray fluorescence (XRF) were close to those in the starting solutions, indicating a proper metal incorporation in the

(8) (a) López-Sánchez, J. A.; Lennon, D. *Appl. Catal., A* **2005**, *291*, 230–237. (b) Segura, Y.; López, N.; Pérez-Ramírez, J. *J. Catal.* **2007**, *247*, 383–386. (c) Azizi, Y.; Petit, C.; Pitchon, V. *J. Catal.* **2008**, *256*, 338–344. (d) Nikolaev, S. A.; Smirnov, V. V. *Catal. Today* **2009**, *147S*, S336–S341.

(9) Studt, F.; Abild-Pedersen, F.; Bligaard, T.; Sørensen, R. Z.; Christensen, C. H.; Nørskov, J. K. *Science* **2008**, *320*, 1320–1322.

(10) (a) Rodríguez, C.; Marchi, A. J.; Borgna, A.; Romeo, E.; Monzón, A. *Stud. Surf. Sci. Catal.* **2001**, *139*, 37–44. (b) Abelló, S.; Verboekend, D.; Bridier, B.; Pérez-Ramírez, J. *J. Catal.* **2008**, *259*, 85–95.

(11) (a) Wehrli, J. T.; Thomas, D. J.; Wainwright, M. S.; Trimm, D. L.; Cant, N. W. *Appl. Catal.* **1990**, *66*, 199–208. (b) Wehrli, J. T.; Thomas, D. J.; Wainwright, M. S.; Trimm, D. L.; Cant, N. W. *Appl. Catal.* **1991**, *70*, 253–262. (c) Bridier, B.; López, N.; Pérez-Ramírez, J. *J. Catal.* **2010**, *269*, 80–92.

(12) Abelló, S.; Pérez-Ramírez, J. *Adv. Mater.* **2006**, *18*, 2436–2439.

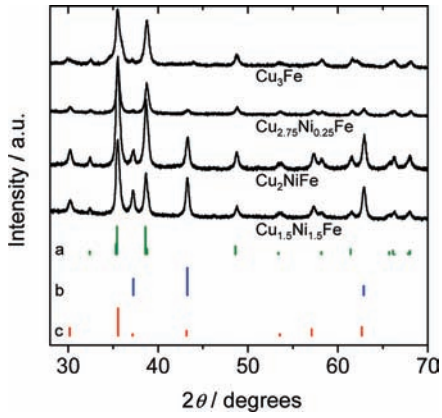

Figure 1. X-ray diffraction patterns of the mixed $Cu_{3-x}Ni_xFe$ oxides. Crystalline phases: (a) CuO; (b) NiO; (c) spinel.

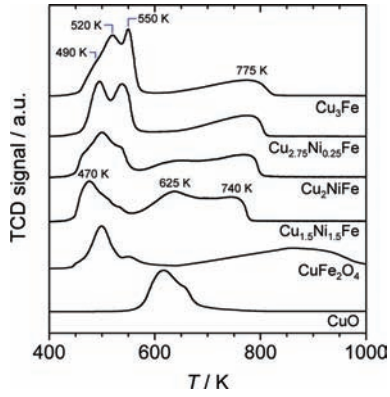

Figure 2. Temperature-programmed reduction with hydrogen of the mixed $Cu_{3-x}Ni_xFe$ oxides. Reference samples: CuO and $CuFe_2O_4$.

precipitates. The solids were calcined at 873 K, and the resulting mixed oxides were characterized by X-ray diffraction (XRD), N_2 adsorption, temperature-programmed reduction with hydrogen (H_2-TPR), and X-ray photoelectron spectroscopy (XPS). Figure 1 shows the XRD patterns of the $Cu_{3-x}Ni_xFe$ oxides. The binary Cu_3Fe shows tenorite (CuO) as the main phase and $CuFe_2O_4$ spinel as the secondary phase. On the basis of the Cu_3Fe stoichiometry, only 17% of copper is as $CuFe_2O_4$ and the remaining 83% is as CuO. The $CuFe_2$ sample prepared by the same coprecipitation method and calcined at 873 K yielded $CuFe_2O_4$ as the only crystalline phase.

Progressive replacement of Cu by Ni led to the appearance of NiO reflections in the Cu_2NiFe and $Cu_{1.5}Ni_{1.5}Fe$ samples, coexisting with CuO and the spinel phases. In nickel-rich samples, the spinel phase likely comprises $CuFe_2O_4$ and $NiFe_2O_4$. However, these phases cannot be distinguished, as they have identical diffraction patterns. Replacement of copper by nickel did not produce noticeable changes in the particle size of copper oxide. Application of the Scherrer equation in the (111) reflection of CuO at 38.7° 2θ led to crystallite sizes in the narrow range of 15−18 nm for the different values of x. The average crystallite size of NiO experienced a slight increase from 17 nm in Cu_2NiFe to 21 nm in $Cu_{1.5}Ni_{1.5}Fe$.

The reducibility of the $Cu_{3-x}Ni_xFe$ oxides revealed the intimate metal interaction in these compounds. The H_2-TPR profiles of a series of samples are shown in Figure 2. The binary Cu_3Fe oxide presents different hydrogen consumptions: a shoulder at 490 K and three peaks at 520, 550, and 775 K. By comparison with reference $CuFe_2O_4$ and CuO samples, the feature at 490 K is attributed to reduction of the copper ferrite spinel to metallic copper and iron oxide, while the peaks at 520 and 550 K are due to reduction of copper oxide. The presence of iron shifts the reduction of copper(II) oxide to ca. 100 K lower temperature with respect to pure CuO. Nitta et al.[13] also observed CuO reduction at low temperature (ca. 473 K) in $Fe-Cu/SiO_2$ catalysts. The broad peak at 775 K in Cu_3Fe is due to the reduction of iron oxide to metallic iron. Metallic copper shifts iron oxide reduction to lower temperature, from ca. 860 K in $CuFe_2O_4$ to 775 K in Cu_3Fe. This has been associated with the spillover of hydrogen atoms dissociated on copper to the iron oxide.[14] Partial replacement of copper by nickel from $x = 0.25$ (Cu/Ni = 11) to 1.5 (Cu/Ni = 1) further shifts the reducibility of CuO to lower temperature in relation to the Ni-free oxide, down to 470 K in $Cu_{1.5}Ni_{1.5}Fe$. The shift in CuO reduction by Ni^{2+} and Fe^{3+} is tentatively attributed to the intimate interaction between the metals forming a solid solution. This is supported by X-ray diffraction, as the reflections of copper(II) oxide appear at higher 2θ in $Cu_{3-x}Ni_xFe$ than in pure CuO, indicating smaller cell parameters. Both Ni^{2+} (0.69 Å) and Fe^{3+} (0.64 Å) are smaller than Cu^{2+} (0.73 Å), and their eventual incorporation in the CuO structure causes a slight contraction of the lattice (Figure SI1, Supporting Information). In the presence of both Cu and Ni, the reduction of iron oxide occurred at a lower temperature (740 K) than with Cu only (775 K). The hydrogen consumption due to reduction of nickel(II) oxide starts to be visible in the profile of Cu_2NiFe (broad peak at 625 K). In this composition, distinct NiO reflections were detected by X-ray diffraction. The reducibility of NiO is also catalyzed by metallic copper,[10a,15] as pure nickel(II) oxide is typically reduced above 700 K. The above observations point to the formation of intermetallic compounds in the $Cu_{3-x}Ni_xFe$ samples, which can have a beneficial influence on their hydrogenation performance (vide infra).

Bulk characterization of the $Cu_{3-x}Ni_xM^{3+}$ system presents differences if aluminum is the trivalent metal (M^{3+}) instead of iron. This is illustrated by comparison of the $Cu_{2.75}Ni_{0.25}Al$ and $Cu_{2.75}Ni_{0.25}Fe$ oxides. As expected from our previous study with the binary Cu_3Al oxide,[11c] the XRD pattern of the Al-containing oxides calcined at 873 K only showed tenorite, CuO (Figure SI2a, Supporting Information), as crystallization of the $CuAl_2O_4$ spinel requires higher calcination temperatures. The H_2-TPR profiles (Figure SI2b) show that the reduction of CuO in $Cu_{2.75}Ni_{0.25}Al$ does not display the low-temperature contribution below 500 K, suggesting that the intimate metal interaction observed in $Cu_{2.75}Ni_{0.25}Fe$ cannot be attained with aluminum.

The above differences in bulk characterization are surpassed in importance by surface analysis results using X-ray photoelectron spectroscopy. As shown in Table 1, while the bulk metal ratios in both samples are equivalent, they present striking differences in surface composition. $Cu_{2.75}Ni_{0.25}Al$ experiences a marked surface segregation of aluminum, while copper and nickel are enriched toward the center of the particle. Only 12% of the total copper amount (Cu_s/Cu_b) and 17% of the total nickel amount (Ni_s/Ni_b) are located at the Al-rich surface. This is in contrast with the much higher surface exposure of copper and nickel in $Cu_{2.75}Ni_{0.25}Fe$: i.e., $Cu_s/Cu_b = 71\%$ and $Ni_s/Ni_b = 76\%$, respectively. We have previously observed strong surface

(13) Nitta, Y.; Hiramatsu, Y.; Okamoto, Y.; Imanaka, T. *Stud. Surf. Sci. Catal.* **1991**, *63*, 103–112.
(14) Kameoka, S.; Tanabe, T.; Tsai, A. P. *Catal. Lett.* **2005**, *100*, 89–93.
(15) Naghash, A. R.; Etsell, T. H.; Xu, S. *Chem. Mater.* **2006**, *18*, 2480–2488.

Table 1. Characterization Data of Selected Oxides prior to Any Reductive Treatment

	molar Cu/Ni/(Fe,Al) ratio				
sample	bulk (b)[a]	surface (s)[b]	Cu_s/Cu_b, %	Ni_s/Ni_b, %	S_{BET},[c] $m^2\ g^{-1}$
$Cu_{2.75}Ni_{0.25}Fe$	2.44/0.24/1	1.74/0.18/1	71	76	35
$Cu_{2.75}Ni_{0.25}Al$	2.97/0.28/1	0.35/0.05/1	12	17	89

[a] Determined by XRF. [b] Determined by XPS. [c] Total surface area, N_2 adsorption.

segregation of aluminum in binary Ni_3Al[10b] and Cu_3Al[11c] catalysts. Despite their efficient performance in propyne hydrogenation, this feature was regarded as an important drawback, as the concentration of nickel and copper sites exposed to the reactant mixture is limited and therefore the overall metal content in the sample is ineffectively utilized in the reaction. The first task accomplished in this work for designing a better hydrogenation catalyst was to increase the fraction of exposed copper in the Fe-containing precursor by a factor of 5 with respect to the Al-containing analogue.

Prior to the hydrogenation tests, the catalysts were treated in 5 vol % H_2/He at 773 K. At this temperature, both copper and nickel oxides are fully reduced (Figure 2). The H_2-TPR profile of the in situ reduced sample showed a single peak at 870 K attributed to the reduction of remaining iron oxide (Figure SI3a). The XRD patterns of the reduced samples showed reflections of Cu, Fe, and Fe_3O_4 (Figure SI3b), as well of Ni (for $x > 1$ in $Cu_{3-x}Ni_xFe$). The XPS results in Table 1 belong to the calcined samples: i.e., the relative surface concentration of the metals could have changed upon reduction. Previous XPS characterization of binary Ni−Al[10b] and Cu−Al[11c] catalysts rendered similar metal distributions in calcined and ex situ reduced forms. For this reason, we assume that the relative surface metal concentration in the calcined and reduced Cu−Ni−Fe and Cu−Ni−Al samples does not differ significantly. However, a precise assessment of eventual changes in metal distribution upon reduction of the oxide precursors would require dedicated analyses using, for example, in situ XPS. In any case, the more even distribution of Cu and Ni in the Fe-containing catalyst compared to the Al-containing catalyst in reduced forms can be expected by attending to computed surface segregation energies (E_{segr}) in transition-metal alloys.[16] The pairs Cu−Fe and Ni−Fe, with Cu or Ni as host and Fe as solute, resulted in moderate antisegregation: i.e., slight surface enrichment of iron. For the pair Cu−Ni, moderate nickel enrichment was computed. These predictions are in good agreement with the XPS results of the $Cu_{2.75}Ni_{0.25}Fe$ oxide in Table 1.

Catalytic tests in alkyne hydrogenation comprised the investigation of the influence of temperature, the H_2/alkyne ratio, and the presence of excess alkene in the feed. We primarily aimed at simulating tail-end conditions: i.e., the most common process used in industry to hydrogenate highly unsaturated compounds in C2 and C3 cuts of steam cracking.[1,2,5] Figure 3 shows the influence of the degree of copper replacement by nickel in the ternary $Cu_{3-x}Ni_xFe$ catalyst on the propyne conversion and selectivity to products in a feed mixture of $H_2/C_3H_4 = 3$ at 523 K. The sample Cu_3Fe shows selectivity to propene of 70% at a full degree of propyne conversion; oligomers comprise the only byproduct (30% selectivity): i.e., no propane was formed. Equivalent results were achieved over Cu_3Al,[11c] confirming the ability of copper-based catalyst to activate the undesirable

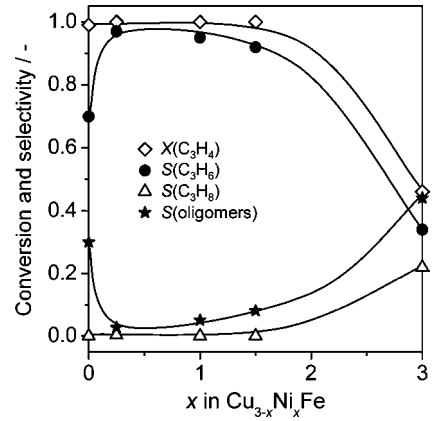

Figure 3. Propyne conversion and selectivity to propene, propane, and oligomers vs the degree of copper replacement by nickel in the $Cu_{3-x}Ni_xFe$ catalysts. Conditions: $C_3H_4/H_2/He = 2.5/7.5/90$, $T = 523$ K, $SV = 16\,800$ $cm^3\ g^{-1}\ h^{-1}$, and $P = 1$ bar.

oligomerization pathway leading to green oil. Addition of nickel boosts the propene selectivity, practically suppressing any oligomer production. The best catalyst under these conditions was $Cu_{2.75}Ni_{0.25}Fe$, with 97% selectivity to the olefin. The propene selectivity slightly decreases to 95% and 90% upon increasing the Ni content in the catalyst ($x = 1$ and 1.5, respectively). However, the propene selectivity remains very high for a wide range of nickel contents. In the other extreme, the binary Ni_3Fe is a very poor catalyst, displaying a propene selectivity of 35% at a relatively low degree of propyne conversion (<50%). The selectivity to oligomers exceeds 40%, and propane is produced with a selectivity >20%.

The high alkene selectivity exhibited by copper and the remarkable effect of nickel in the catalyst can be explained with the aid of mechanistic aspects elaborated elsewhere using density functional theory calculations.[11c] In clear analogy with Au nanoparticles,[8b] the selective character of copper in partial alkyne hydrogenation is attributed to its high thermodynamic factor, defined as the difference between the binding energy of the triple and double bonds. Propyne adsorbs weakly on copper (−0.17 eV on Cu(111)), while propene adsorption is endothermic. Dissociation of molecular hydrogen on Cu(111) is marginally endothermic (0.16 eV) and is hindered by a large barrier of 0.83 eV. Since H_2 dissociation is the rate-determining step on copper,[11c] the hydrogen coverage is very low and therefore extensive oligomerization takes place and the alkane production is zero. Addition of nickel enhances the hydrogen coverage on the catalyst, as H_2 dissociation on Ni(111) is exothermic (−0.75 eV) and has a barrier of 0.17 eV: i.e., very low compared with copper. The availability of hydrogen atoms generated on Ni sites, which can spill over to closely interacting Cu sites, suppresses undesired oligomerization on the latter metal and thus sharp alkyne conversion to the alkene is attained. Above a certain nickel content the alkene selectivity is lowered, since the partial hydrogenation is kinetically favored over Cu vs Ni. The barriers for the first ($C_3H_4 + H \rightarrow C_3H_5$) and second ($C_3H_5 + H \rightarrow C_3H_6$) hydrogenation steps are much lower on clean Cu(111) (0.41 and 0.45 eV, respectively) than on clean Ni(111) (0.89 and 0.65 eV, respectively).[11c] In addition, nickel is prone to generate subsurface hydrogen and NiH_x hydrides, which are known to catalyze unselective processes.[17] Advantageously,

(16) Ruban, A. V.; Skriver, H. L.; Nørskov, J. K. *Phys. Rev. B* **1999**, *59*, 15990–16000.

(17) Johnson, A. D.; Daley, S. P.; Utz, A. L.; Ceyer, S. T. *Science* **1992**, *257*, 223–225.

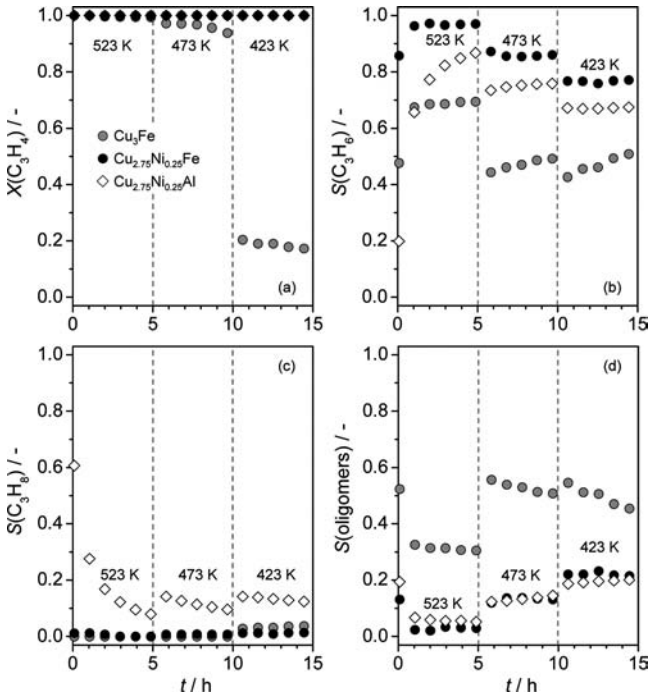

Figure 4. Propyne conversion (a) and selectivity to propene (b), propane (c), and oligomers (d) vs time over selected catalysts at different temperatures. Conditions: $C_3H_4/H_2/He = 2.5/7.5/90$, $SV = 16\,800$ cm^3 g^{-1} h^{-1}, and $P = 1$ bar.

hydride formation is not favored on pure copper under relevant conditions in partial alkyne hydrogenation.

Figure 4 shows the propyne hydrogenation performance vs temperature over the binary Cu_3Fe, the optimal $Cu_{2.75}Ni_{0.25}Fe$, and the aluminum analogue $Cu_{2.75}Ni_{0.25}Al$ catalysts. The Ni-doped Cu−Fe catalyst presents much higher propene selectivity (Figure 4b) than the undoped Cu−Fe catalyst in the whole temperature range, due to the suppressed reaction channel leading to oligomers (Figure 4d). The propene selectivity decreases with a decrease in temperature due to less effective H_2 dissociation and thus lower hydrogen coverage, which ultimately switches the reaction from the preferential formation of the alkene to the preferential formation of oligomers. Copper-based catalysts are known to deactivate below 450 K due to extensive green oil formation.[11] This is confirmed by the drop of C_3H_4 conversion over Cu_3Fe from ca. 100% at 473 K to 20% at 423 K (Figure 4a). However, the C_3H_4 conversion over $Cu_{2.75}Ni_{0.25}Fe$ is kept at 100% even at 423 K due to the effect of nickel in increasing the H coverage. The positive impact of nickel doping to attain an increased alkene selectivity by decreased oligomerization is also observed in the Cu−Al system. Both $Cu_{2.75}Ni_{0.25}Fe$ and $Cu_{2.75}Ni_{0.25}Al$ catalysts display full propyne conversion in the temperature range investigated (Figure 4a). However, the iron-containing catalyst is more selective to propene in the whole temperature range. The selectivity to oligomers over both catalysts is similar, but $Cu_{2.75}Ni_{0.25}Al$ leads to some overhydrogenation. As shown in Figure 4c, the propane selectivity on $Cu_{2.75}Ni_{0.25}Al$ is 10−15% in contrast with the zero propane production on $Cu_{2.75}Ni_{0.25}Fe$. This is attributed to the lower surface exposure of copper in the Al-containing catalysts, which confirms the crucial role of iron on the catalytic performance by promoting an enhanced amount of copper available on the catalyst surface.

An important characteristic of any partial hydrogenation catalyst is the dependence of the alkene selectivity and alkyne

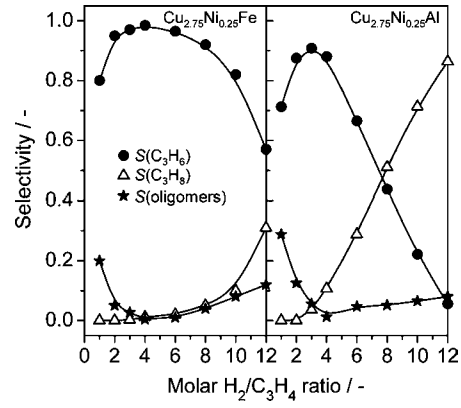

Figure 5. Selectivity to propene, propane, and oligomers vs the molar H_2/C_3H_4 ratio in the feed over $Cu_{2.75}Ni_{0.25}Fe$ and $Cu_{2.75}Ni_{0.25}Al$ catalysts. Conditions: 2.5 vol % C_3H_4 and 2.5−30 vol % H_2, balance He, $T = 523$ K, $SV = 16\,800$ cm^3 g^{-1} h^{-1}, and $P = 1$ bar.

conversion on the feed hydrogen-to-alkyne ratio. From the point of view of process robustness, it is highly desirable (and challenging) to keep a high alkene selectivity in a wide range of inlet partial hydrogen pressures in order to accommodate possible fluctuations in the feed coming from the steam cracker. Typical Pd-based catalysts applied in tail-end hydrogenation yield acceptable propene selectivity in the narrow range of H_2/alkyne = 1.5−2[1] and include continuous feeding of carbon monoxide (1−10 ppm CO) as selectivity enhancer.[18] A slight excess of hydrogen over the stoichiometric ratio of 1 is required to enhance the alkyne conversion and reduce oligomers or green oil, while ratios >2 lead to extensive alkane production due to the occurrence of the unselective palladium hydride phase.[3b,7c−e] Figure 5 shows the selectivity to products at 523 K and H_2/C_3H_4 ratios ranging from 1 to 12 over $Cu_{2.75}Ni_{0.25}Fe$ and $Cu_{2.75}Ni_{0.25}Al$. The propyne conversion was 100% under all conditions. In contrast to palladium catalysts, $Cu_{2.75}Ni_{0.25}Fe$ is tolerant to the partial H_2 pressure, so that a C_3H_6 selectivity >90% was attained in the range of $H_2/C_3H_4 = 2-6$ with a maximum of 98.5% at a ratio of 4. The stoichiometric ratio $H_2/C_3H_4 = 1$ decreases the C_3H_6 selectivity to 80% at the expenses of oligomers. A large hydrogen excess ($H_2/C_3H_4 > 8$) activates the reaction pathway toward the alkane, with oligomers as the secondary byproduct. The C_3H_6 selectivity over $Cu_{2.75}Ni_{0.25}Al$ did not exceed the value of 90% at optimal H_2/C_3H_4 ratios. Most important, the window of H_2/C_3H_4 ratios for optimal alkene selectivity was narrower compared to $Cu_{2.75}Ni_{0.25}Fe$. Specifically, the drop of propene selectivity at high H_2/C_3H_4 ratios was much steeper on $Cu_{2.75}Ni_{0.25}Al$ and, consequently, the propane selectivity was >50% at $H_2/C_3H_4 \geq 8$. The higher hydrogen acceptance of $Cu_{2.75}Ni_{0.25}Fe$ (flatter dependence of $S(C_3H_6)$ vs the H_2/C_3H_4 ratio) is tentatively attributed to the lower nickel segregation on the surface and increased Cu−Ni interaction associated with the presence of iron. The remarkable hydrogen acceptance of $Cu_{2.75}Ni_{0.25}Fe$ can be of great practical relevance, possibly enabling its application in front-end partial alkyne hydrogenation, in which a large H_2 excess is present.[1] The latter process is less popular than tail-end hydrogenation because there is the danger of thermal runaway if the composition of the feed gas fluctuates. Therefore, the implementation of Pd-based catalysts in front-end alkyne hydrogenation requires increasing the inlet CO concentration (in the range of 150−5000 ppm) to moderate the reaction toward

(18) Schwab, E. BASF, personal communication, 2007.

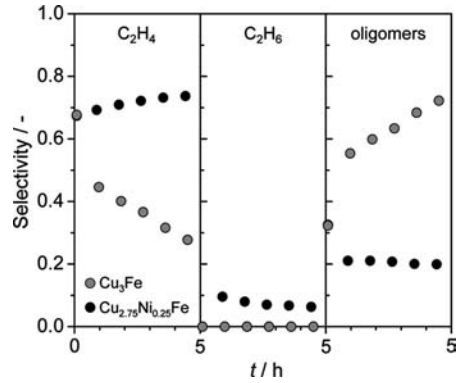

Figure 6. Selectivity to ethene (left), ethane (center), and oligomers (right) vs time over Cu_3Fe and $Cu_{2.75}Ni_{0.25}Fe$ catalysts. Conditions: $C_3H_4/H_2/He = 2.5/7.5/90$, $T = 523$ K, $SV = 16\,800$ cm^3 g^{-1} h^{-1}, and $P = 1$ bar.

the olefin by suppressing PdH formation. The CO concentration decreases in the course of the cycle time as the buildup of carbonaceous deposits occurs, and therefore a control system linked with the degree of activity and alkene selective must be installed. The ternary Cu−Fe−Ni catalyst requires no CO feeding to approach 100% propene selectivity. This aspect represents a significant process simplification with respect to today's reactor technology.

We also conducted a 30 h test over the best catalysts, $Cu_{2.75}Ni_{0.25}Fe$, using a reaction mixture with $H_2/C_3H_4 = 3$ and $C_3H_6/C_3H_4 = 5.4$ at 523 K. This feed aims at simulating realistic conditions in hydrogenation, in which the alkyne to be selectively hydrogenated takes part of a mixture containing an excess of olefin. The olefin selectivity was 100% at a full degree of propyne conversion, and the catalyst was remarkably stable. Our results are in line with Wehrli et al.,[11a] who observed that the alkene selectivity in propyne hydrogenation over Cu/SiO_2 increased as the amount of propylene in the feed increased.

The gas-phase hydrogenation of ethyne was studied over selected catalysts to verify that the remarkable selectivity enhancement applies to other acetylenic compounds. The tests were carried at 523 K in a feed mixture with $H_2/C_2H_2 = 3$. The degree of ethyne conversion was 100%. As shown in Figure 6, the ethene selectivity is largely increased in the ternary $Cu_{2.75}Ni_{0.25}Fe$ compared to the binary Cu_3Fe. The ethene selectivity was stable at 70−75% over $Cu_{2.75}Ni_{0.25}Fe$. In contrast, the ethene selectivity over Cu_3Fe dropped drastically from the initial value of 68% to 20% during 5 h on stream at the expense of a markedly increased selectivity to oligomers. Due to the presence of nickel, $Cu_{2.75}Ni_{0.25}Fe$ led to some overhydrogenation (C_2H_6 selectivity $\leq$10%), while the production of ethane was zero over Cu_3Fe. The same explanation of the enhanced alkene selectivity in propyne hydrogenation upon nickel addition in the multimetallic catalysts (enhanced H coverage leading to minimized oligomerization) applies to ethyne hydrogenation. The lower alkene selectivity achieved over the catalysts with ethyne as compared to propyne is a general feature of partial hydrogenation catalysts.[2b,3b,10b] This is due to the more pronounced oligomerization with ethyne. The selectivity to oligomers is known to decrease for higher alkynes due to steric interferences in the C−C bond-forming step.[3b] The ethene selectivity over $Cu_{2.75}Ni_{0.25}Fe$ in ethyne + ethene mixtures ($H_2/C_2H_2 = 3$ and $C_2H_4/C_2H_2 = 5.4$) at 523 K reached 80% and was stable during the 30 h test. The dependence of the product distribution on the feed H_2/C_2H_2 ratio shows parallels with that of propyne hydrogenation: i.e., the optimal alkene selectivity is obtained at similar feed hydrogen-to-alkyne ratios (2−4) and the alkene selectivity remains high in a broad range of inlet partial H_2 pressures (Figure SI4, Supporting Information).

In summary, we have discovered a novel family of ternary $Cu_{3-x}Ni_xFe$ catalysts with 100% propene selectivity and 80% ethene selectivity in the gas-phase hydrogenation of propyne and ethyne, respectively. For comparative purposes, the hydrogenation of propyne and ethyne was evaluated in the same reactor setup over a nonpromoted 1 wt % Pd/Al_2O_3 catalyst under typical conditions for palladium-based catalysts (H_2/alkyne = 1.5 and $T = 348$ K). The selectivity to propylene and ethylene amounted to <30%, putting in clear perspective the achievement with the ternary catalytic system. Copper is intrinsically selective to the alkene and was used as the base hydrogenation metal. However, its poor H_2 splitting ability activates the oligomerization pathway. Addition of nickel cures this deficiency due to the more facile H_2 dissociation on this metal, increasing the hydrogen coverage and thus minimizing the undesired oligomerization. The intimate contact between Cu and Ni in the catalyst, evidenced by characterization of the corresponding oxide precursors, appears to be essential for the catalyst to display the unique cooperative effect. An optimal amount of nickel maximizes the alkene selectivity ($x \approx 0.25$), although the window of nickel contents for a remarkable selective behavior is pretty broad (Figure 3). In any case, it is seen that a gradual increase of nickel uncovers undesired processes characteristic of pure nickel:[10] i.e., alkane production by overhydrogenation and oligomerization due to extensive C−C cleavage. The role of iron as the third metal in the Cu−Ni−Fe catalyst should not be underestimated, as equivalent catalytic results with the analogous Cu−Ni−Al system could not be realized. In contrast to the marked metal segregation in the presence of aluminum, iron enhances the fraction of surface copper and nickel sites in the oxide precursor. It should be stressed that assessing the metal distribution during reduction of the oxides and, principally, along the catalytic reaction are important milestones for future investigations and would require the application of surface-sensitive in situ and operando methods.

The implementation of the ternary catalytic system in tail-end alkyne hydrogenation is promising, as it brings a handful of advantages with respect to the state-of-the-art promoted Pd catalysts: (i) it does not contain noble metals; (ii) it does not require continuous CO feeding as selectivity enhancer; (iii) the remarkable alkene selectivity is increased when excess alkene is fed to the reactor; (iv) since ca. 100% alkene selectivity is attained (in the case of propyne hydrogenation), separation costs of the olefin and byproduct downstream of the hydrogenation reactor are substantially reduced; (v) green oil formation (main cause for deactivation) is largely minimized and even suppressed and therefore long cycle times and catalyst lifetime can be expected; (vi) the catalyst operates selectively in a broad range of H_2/alkyne ratios, opening room for its application in front-end hydrogenation. The only aspect to take into consideration is the different higher operating temperature of $Cu_{3-x}Ni_xFe$ (523 K) in comparison to that for Pd-based systems (293−393 K).[1] This aspect, which is directly linked to the easier dissociation of hydrogen on palladium, does not enable a straightforward drop-in solution of the $Cu_{3-x}Ni_xFe$ catalysts in current deacetylenization reactors. However, we firmly think that the incentive to bridge this gap of temperature is high, taking into consideration the remarkable alkene selectivity and the process simpli-

fications stressed above. The ternary catalyst should be subjected to detailed kinetic studies, investigating among others the influence of total pressure and space velocity.

Finally, this paper dealt with the alkyne hydrogenation in the gas phase, namely for purification of olefin streams in C2 and C3 cuts. In the mid term, we plan to evaluate the performance of the ternary Cu−Ni−Fe catalysts in liquid-phase (chemo)selective hydrogenation of acetylenic compounds. Such a family of reactions is of high relevance in organic synthesis for the manufacture of fine chemicals,[19] and the Lindlar catalyst[20] (5 wt % $Pd/CaCO_3$ poisoned by lead and quinoline) is typically applied. The benefits of the $Cu_{3-x}Ni_xFe$ system could target not only the potential selectivity improvement but also a much lower catalyst cost by suppressing the use of the noble metal and the various poisoning steps.

Acknowledgment. We thank the Spanish MICINN (CTQ2006-01562PPQ, CTQ2009-09824/PPQ, and Consolider-Ingenio 2010, CSD2006-0003), the Catalan Government (2009-SGR-461), and the ICIQ Foundation for funding part of this work. Prof. N. López is acknowledged for fruitful discussions.

Note Added after ASAP Publication. The authors' affiliations were not correctly indicated in the version of this article published ASAP February 23, 2010. The corrected version was published February 25, 2010.

Supporting Information Available: Figures giving characterization results by X-ray diffraction and temperature-programmed reduction with hydrogen and catalytic results of propyne and ethyne hydrogenation at different feed H_2/alkyne ratios. This material is available free of charge via the Internet at http://pubs.acs.org.

JA9101997

(19) Semagina, N.; Renken, A.; Kiwi-Minsker, L. *J. Phys. Chem. C* **2007**, *111*, 13933–13937. Rebrov, E. V.; Klinger, E. A.; Berenguer-Murcia, A.; Sulman, E. M.; Schouten, J. C. *Org. Process Res. Dev.* **2009**, *13*, 991–998. Anderson, J. A.; Mellor, J.; Wells, R. P. K. *J. Catal.* **2009**, *261*, 208–216.

(20) Lindlar, H. *Helv. Chim. Acta* **1952**, *35*, 446–450.